JOURNAL OF VIROLOGY, Aug. 2010, p. 7880–7885 Vol. 84, No. 15
0022-538X/10/$12.00 doi:10.1128/JVI.00486-10

NOTES

The Proteasome Inhibitor Velcade Enhances rather than Reduces Disease in Mouse Hepatitis Coronavirus-Infected Mice▽

Matthijs Raaben,[1]† Guy C. M. Grinwis,[2] Peter J. M. Rottier,[1] and Cornelis A. M. de Haan[1]*

Virology Division, Department of Infectious Diseases and Immunology, Faculty of Veterinary Medicine, Utrecht University, Utrecht, Netherlands,[1] and Pathology Division, Department of Pathobiology, Utrecht University, Utrecht, Netherlands[2]

Received 4 March 2010/Accepted 7 May 2010

Many viruses, including coronaviruses (CoVs), depend on a functional cellular proteasome for efficient infection *in vitro*. Hence, the proteasome inhibitor Velcade (bortezomib), a clinically approved anticancer drug, shown in an accompanying study (M. Raaben et al., J. Virol. 84:7869–7879, 2010) to strongly inhibit mouse hepatitis CoV (MHV) infection in cultured cells, seemed an attractive candidate for testing its antiviral properties *in vivo*. Surprisingly, however, the drug did not reduce replication of the virus in mice. Rather, inhibition of the proteasome caused enhanced infection with lethal outcome, calling for caution when using this type of drug during infection.

The cellular proteasome is a central actor in protein degradation in eukaryotes (48). This barrel-shaped cytosolic complex has at least three peptidase activities (i.e., caspaselike, trypsinlike, and chymotrypsinlike activities), which are mediated by different subunits (11, 14, 15). Proteasomal degradation is an important mechanism to control protein homeostasis, thereby regulating various basic cellular processes, including cell cycle regulation, cell adhesion, gene transcription, and apoptosis (12, 19, 28, 29, 37).

Because proteasome inhibitors induce apoptosis preferentially in tumor cells, they represent a novel class of drugs in anticancer therapy (10, 16, 30, 42). One of these drugs, Velcade (Bortezomib; formerly known as PS-341, LDP-341, and MLM341), selectively blocks the chymotrypsinlike activity of the catalytic core of the proteasome 20S subunit (1, 2). Velcade has been clinically approved for the treatment of multiple myelomas and mantle cell lymphoma (17, 18), while it also displays anticancer activity against a range of different human malignancies in cell culture and in animal models, including myeloma, pancreatic cancer, lung cancer, prostate cancer, chronic lymphocytic leukemia, and colon cancer (7, 31–33, 40, 41).

Viruses are obligatory intracellular parasites that exploit the host cell for generating their progeny virions. A functional cellular proteasomal system has been shown to be critical for many viruses, including coronaviruses (CoVs), at different stages of their life cycle (8, 20, 23, 24, 39, 43, 50). Thus, in addition to their potential as anticancer drugs, proteasome inhibitors also appear to be promising antiviral agents (39, 45). Supporting this idea, proteasome inhibitors have been shown to protect against coxsackievirus-induced myocarditis and to prolong the survival of mice inoculated with Epstein-Barr virus-transformed B cells (13, 51). However, proteasome inhibitors have also been shown to exhibit immunosuppressive properties. They can, for example, alter TLR4-induced dendritic cell activation and interfere with the immunological functions of T cells (4, 27). Furthermore, cancer patients treated with Velcade demonstrate increased reactivation of varicella herpes

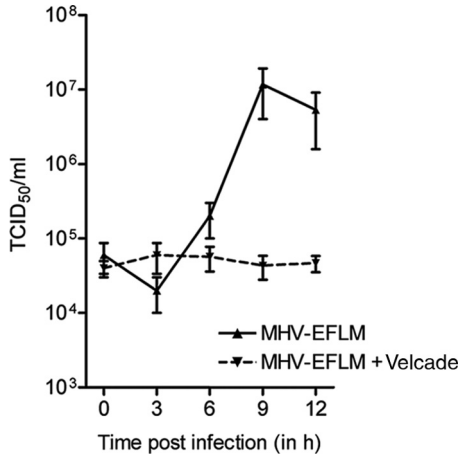

FIG. 1. Velcade inhibits MHV infection in cell culture. LR7 cells were pretreated with 10 μM Velcade or mock treated for 1 h. Subsequently, the cells were infected with MHV-EFLM (multiplicity of infection of 1) in the presence or absence of 10 μM Velcade. After 1 h, the inoculum was removed, and the cells were extensively washed. Incubation was then continued in the absence or presence of Velcade. The virus titers in the culture media at the indicated time points were determined by using a quantal assay and are expressed as $TCID_{50}$ units.

* Corresponding author. Mailing address: Virology Division, Department of Infectious Diseases and Immunology, Faculty of Veterinary Medicine, Utrecht University, Yalelaan 1, 3584 CL Utrecht, Netherlands. Phone: 31 30 2534195. Fax: 31 30 2536723. E-mail: c.a.m.dehaan@uu.nl.

† Present address: Department of Microbiology and Molecular Genetics, Harvard Medical School, 200 Longwood Avenue, Boston, MA 02115-5701.

▽ Published ahead of print on 19 May 2010.

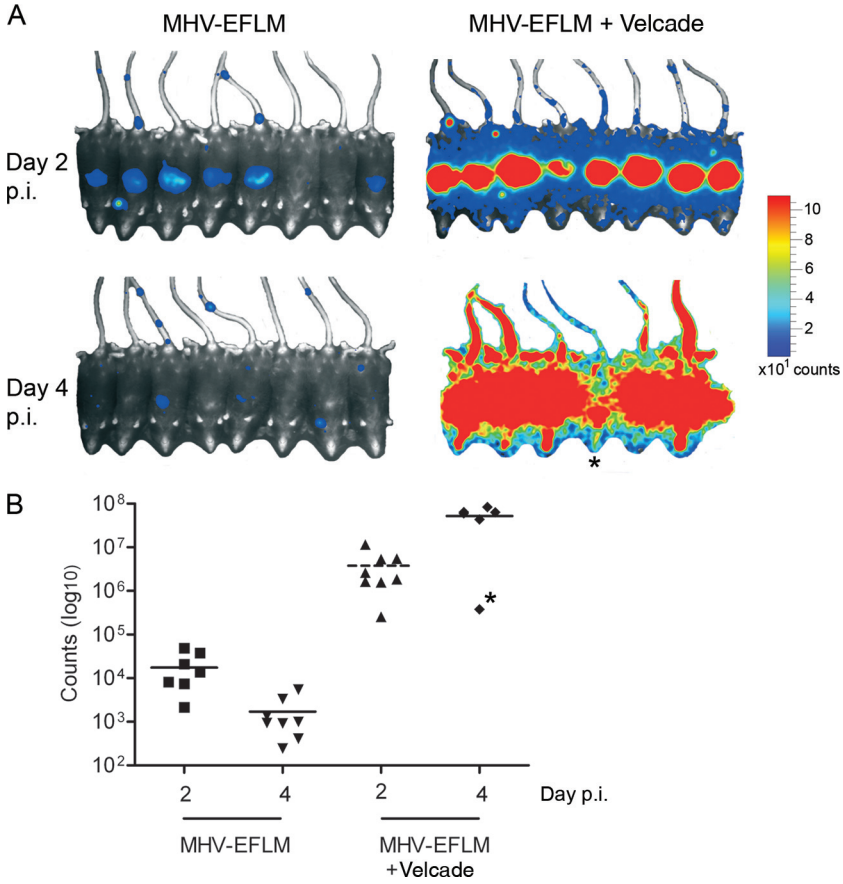

FIG. 2. Bioluminescence imaging of MHV-infected, Velcade-treated mice. Six-to eight-week-old C57BL/6 mice were injected intraperitoneally with Velcade (1 mg/kg) or PBS 30 min prior to inoculation with MHV-EFLM. Treatment with Velcade or PBS was repeated at day 2. Mice were anesthetized and subsequently imaged as described before using a Biospace CCCD camera (35). (A) Mice from each group were imaged simultaneously exactly 5 min after the injection of D-luciferin. Mice were imaged for 10 min on their ventral sides at days 2 and 4 postinfection (p.i.). (B) The bioluminescent signals (expressed as counts) were quantified for each group ($n = 8$) using Photovision software (Biospace Lab). Note that two mice from the Velcade-treated group succumbed to the infection before they could be imaged at day 4, while one mouse (indicated by the asterisk) died during imaging.

zoster virus infections (6, 21, 46). Thus, while playing essential roles in the replication of several viruses, the proteasome is also critically involved in generating an effective antiviral immune response.

In the present study we evaluated the ability of Velcade (obtained from Millennium Pharmaceuticals, Inc.) to inhibit mouse hepatitis virus (MHV) infection in living animals. Previously, we showed that different proteasome inhibitors can dramatically affect the replication of different coronaviruses (CoVs; i.e., MHV, FIPV, and SARS-CoV), as determined by measuring reporter gene expression at different time points postinfection (33a). We confirmed and extended these observations here by evaluating the antiviral effect of Velcade in cell culture by performing a one-step growth curve with MHV-A59 in LR7 mouse fibroblast cells (22). To this end, cells were infected in the absence or presence of 10 μM Velcade (Fig. 1). At the indicated time points, the virus titers in the supernatant were determined by using a quantal assay. In the presence of Velcade, virus production was dramatically affected (Fig. 1), a result that is in agreement with the decrease in virus replication observed previously (33a), whereas cell viability was not affected, as determined by a Wst-1 assay (47).

To investigate whether the proteasome inhibitor Velcade could also inhibit infection *in vivo*, we next used our recently developed bioluminescence imaging (BLI) model to monitor the spatial and temporal progression of MHV infection in living mice (35). To this end, C57BL/6 mice were inoculated intraperitoneally with 10^6 50% tissue culture infective doses ($TCID_{50}$) of MHV-EFLM, which is a recombinant MHV expressing the firefly luciferase (FL) reporter gene. The mice were either pretreated with Velcade in phosphate-buffered saline (PBS) at 1 mg/kg or with an equal volume of PBS. The drug was applied intraperitoneally on days −1 and 2 relative to the time of inoculation with MHV-EFLM. Replication, as measured by determining the amount of *in vivo* FL activity, was assessed by BLI as described previously (35). All mice were imaged for exactly 10 min on their ventral sides. As shown in Fig. 2, treatment of MHV-infected mice with Velcade resulted in a dramatic increase in FL expression. This increase was already significant at day 2 postinfection but developed rapidly

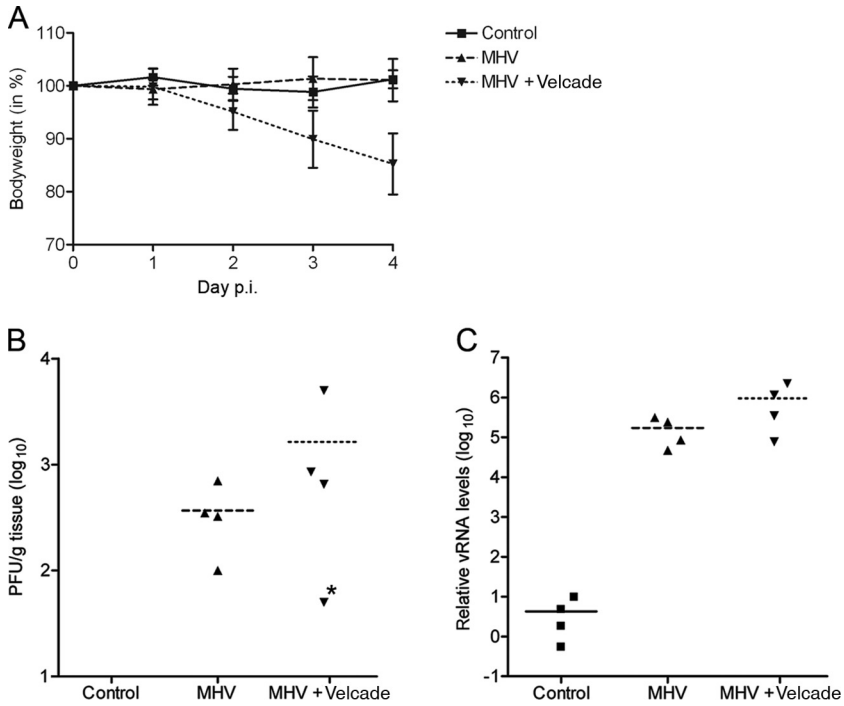

FIG. 3. Velcade enhances MHV pathogenesis in mice. Six- to eight-week-old C57BL/6 mice were injected with Velcade (1 mg/kg) or PBS 30 min prior to infection with MHV-A59. Control animals were not infected and were treated only with Velcade. Treatment with Velcade or PBS was repeated at day 2. (A) Each of the following days the body weights of the animals were measured until the animals were euthanized at day 4. The body weights are expressed as percentages relative to the weights at the beginning of the experiment (day 0 = 100%). (B) The livers were isolated and homogenized as described previously (35). The amount of infectious virus in the homogenates was determined by plaque assays as described previously (35). The virus titers are expressed as PFU/g of tissue (the threshold of detection is 10 PFU/g). Note that the triangle indicated by the asterisk corresponds to a mouse that already succumbed to the infection during the night before day 4. (C) The relative amounts of viral genomic RNA in the liver homogenates were determined by quantitative TaqMan RT-PCR on the 1b region of the MHV genome, as described previously (9).

further during the next 2 days. In sharp contrast, the mock-treated, MHV-infected animals showed a reduction in FL levels from days 2 to 4. Furthermore, the Velcade-treated mice, but not the mock-treated animals, showed severe clinical signs (i.e., weight loss and rough fur), with two mice already succumbing to the infection before day 4 (data not shown). These data strongly suggest that treatment of MHV-infected mice with the proteasome inhibitor Velcade does not inhibit infection but rather enhances it.

To corroborate these results, we subsequently performed an additional experiment in which we used more conventional methods to measure MHV replication in mice. Therefore, C57BL/6 mice were inoculated intraperitoneally with 10^6 $TCID_{50}$ of wild-type MHV-A59. Treatment with Velcade was performed as described above. As an additional control, a group of mice ($n = 4$) was treated with Velcade only. Body weight measurements were performed daily; at day 4 postinfection all of the mice were sacrificed, and the livers were collected to determine the viral loads. The mice infected with MHV but not treated with Velcade and the uninfected Velcade-treated control animals did not show any clinical symptoms. In contrast, the animals infected with MHV and treated with Velcade showed severe clinical signs with a body weight drop at day 4 of ca. 15% relative to their weight at the start of the experiment (Fig. 3A). One mouse in this group already succumbed to the infection at day 3. The viral loads, as measured by determining the PFU and the amounts of viral RNA in the liver homogenates (Fig. 3B and C), were also higher in

FIG. 4. Velcade results in reduced infiltration of immune cells, increased necrosis of hepatocytes, and increased levels of MHV antigen. (A) Isolated liver tissue was fixed in 4% neutral buffered formaldehyde and paraffin embedded. Liver sections were routinely prepared for immunohistochemistry and analyzed for the presence of MHV antigen by staining with the polyclonal anti-MHV serum k135. Representative images are shown for each experimental condition. (B and C) Histopathological effects in the liver (i.e., hepatocellular necrosis and the presence of inflammatory infiltrate) were investigated by staining tissue sections with hematoxylin and eosin (H&E) (B) or staining with an anti-CD3 antibody (C) for identification of T lymphocytes. Representative images are shown. The dashed lines represent the borders of the lesions, while the arrowheads indicate CD3-positive cells. (D) The mRNA expression levels of several chemokines were determined in the liver homogenates by quantitative RT-PCR using Assay-On-Demand reagents (PE Applied Biosystems) as described previously (36). The comparative C_T method was used to determine the fold change for each gene. The housekeeping gene encoding for 18S rRNA was used as a reference in all assays. The levels of TNF-α, CXCL-1, CXCL-2, IFN-β, and IFN-γ are expressed relative to their expression in livers from uninfected control animals. Significant differences ($P < 0.05$) in expression between mock- and Velcade-treated infected mice are indicated by the asterisk.

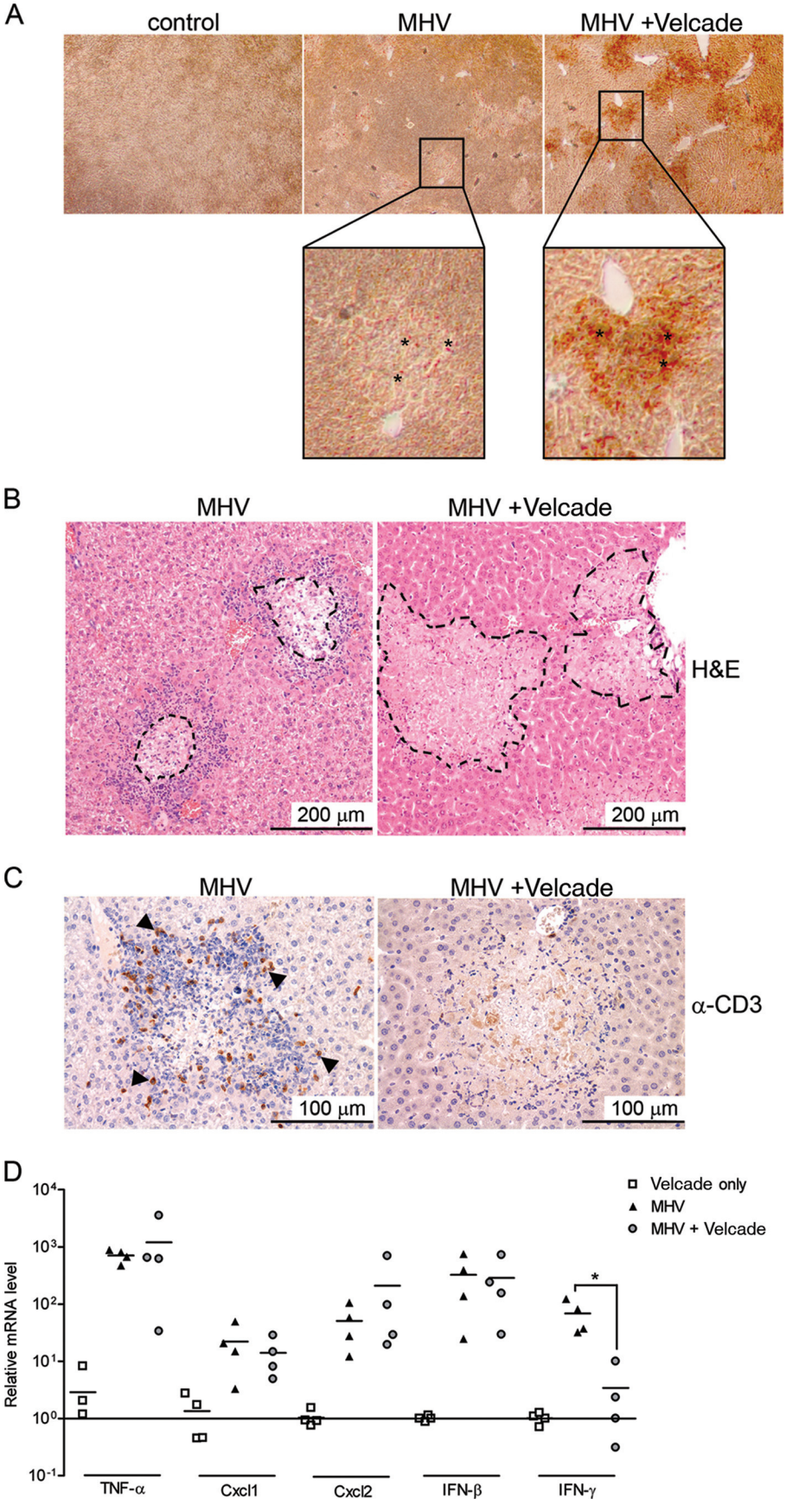

the animals treated with Velcade. However, the viral loads were not elevated as high as might have been expected on the basis of the BLI data.

Next, we analyzed the expression of viral proteins in liver sections of the mice by staining with a polyclonal antiserum (k135) raised against the structural proteins of MHV (38). Although we could detect only moderate staining of viral antigen in the animals infected with MHV, the lesions in MHV-infected mice treated with Velcade appeared to be filled with viral protein (Fig. 4A). In retrospect, these data fit with the much higher expression of the FL reporter gene observed in the treated mice in the BLI experiment (Fig. 2). Histopathologic evaluation of hematoxylin-and-eosin-stained liver sections of the MHV-infected mice showed randomly distributed coagulation necrosis of hepatocytes in mice treated with Velcade and in the control group. However, light microscopic morphometric analysis (using software from Olympus Soft Imaging Solutions Gmbh) of the liver showed a significant ($P < 0.0001$) 3-fold increase in the surface area with necrosis in the MHV-infected mice treated with Velcade compared to the control group ($1.87 \times 10^5\ \mu m^2 \pm 4.1 \times 10^4\ \mu m^2$ versus $5.89 \times 10^4\ \mu m^2 \pm 8.3 \times 10^3\ \mu m^2$, respectively). Moreover, semiquantitative analysis of the inflammatory response showed a markedly reduced presence of leukocytes in the necrotic areas of the liver in the MHV-infected mice treated with Velcade compared to the control animals (Fig. 4B). Immunohistochemical evaluation of the affected areas indicated a reduction in T lymphocytes (Fig. 4C). In agreement with previous results (34), we observed an upregulation of cytokine gene expression (i.e., tumor necrosis factor alpha [TNF-α], CXCL-1, CXCL-2, and beta interferon [IFN-β]) in the livers of MHV-infected mice as determined by quantitative reverse transcription-PCR (RT-PCR). Interestingly, a similar induction of cytokine gene expression was also observed in the MHV-infected animals treated with Velcade, with the exception of the IFN-γ induction (Fig. 4D). This latter observation probably reflects the absence of activated immune cells in the virus-induced lesions. Altogether, we observed that proteasome inhibition during MHV infection results in an accumulation of viral antigen accompanied by the reduced presence of inflammatory cells at the sites of infection, which results in a fatal coagulation necrosis of hepatocytes.

The reduced inflammatory response (most notably, the reduced recruitment of T-lymphocytes) at the sites of MHV infection in the liver indicates that proteasome inhibition abrogates the induction of a protective immune response against MHV. Likewise, it has been shown recently that mice treated with Velcade were more susceptible to lymphocytic choriomeningitis virus infection (3). These observations correspond with the findings of recent studies, which demonstrate that proteasome inhibition promotes apoptosis in primary natural killer cells and dendritic cells (DCs) and inhibits DC maturation (26, 44, 49). In addition, exposure of mice to bortezomib radically impaired murine T-lymphocyte development in the thymus (25) and induced selective apoptosis and decreased Th1 responses among alloreactive T lymphocytes, while leaving unstimulated T cells unaffected (5). The present study shows for the first time that the immunosuppressive effects of the proteasome inhibitor Velcade may have a fatal outcome in mice infected with MHV, indicating that proteasome inhibitors are probably not useful as anti(corona)viral agents. Our results warrant a more in-depth investigation of the use of proteasome inhibitors in a clinical setting since they may result in adverse side effects in virus-infected individuals.

This study was supported by grants from the M. W. Beijerinck Virology Fund (Royal Netherlands Academy of Arts and Sciences) and The Netherlands Organization for Scientific Research (NWO-VIDI-700.54.421) to C. A. M. de Haan.

We thank Marne Hagemeijer and Mijke Vogels for stimulating discussions.

REFERENCES

1. **Adams, J.** 2002. Development of the proteasome inhibitor PS-341. Oncologist **7:**9–16.
2. **Adams, J., and M. Kauffman.** 2004. Development of the proteasome inhibitor Velcade (Bortezomib). Cancer Invest. **22:**304–311.
3. **Basler, M., C. Lauer, U. Beck, and M. Groettrup.** 2009. The proteasome inhibitor bortezomib enhances the susceptibility to viral infection. J. Immunol. **183:**6145–6150.
4. **Berges, C., H. Haberstock, D. Fuchs, M. Miltz, M. Sadeghi, G. Opelz, V. Daniel, and C. Naujokat.** 2008. Proteasome inhibition suppresses essential immune functions of human $CD4^+$ T cells. Immunology **124:**234–246.
5. **Blanco, B., J. A. Perez-Simon, L. I. Sanchez-Abarca, X. Carvajal-Vergara, J. Mateos, B. Vidriales, N. Lopez-Holgado, P. Maiso, M. Alberca, E. Villaron, D. Schenkein, A. Pandiella, and J. San Miguel.** 2006. Bortezomib induces selective depletion of alloreactive T lymphocytes and decreases the production of Th1 cytokines. Blood **107:**3575–3583.
6. **Chanan-Khan, A., P. Sonneveld, M. W. Schuster, E. A. Stadtmauer, T. Facon, J. L. Harousseau, D. Ben-Yehuda, S. Lonial, H. Goldschmidt, D. Reece, R. Neuwirth, K. C. Anderson, and P. G. Richardson.** 2008. Analysis of herpes zoster events among bortezomib-treated patients in the phase III APEX study. J. Clin. Oncol. **26:**4784–4790.
7. **Chauhan, D., T. Hideshima, C. Mitsiades, P. Richardson, and K. C. Anderson.** 2005. Proteasome inhibitor therapy in multiple myeloma. Mol. Cancer Ther. **4:**686–692.
8. **Chen, Y. T., C. H. Lin, W. T. Ji, S. K. Li, and H. J. Liu.** 2008. Proteasome inhibition reduces avian reovirus replication and apoptosis induction in cultured cells. J. Virol. Methods **151:**95–100.
9. **de Haan, C. A., K. Stadler, G. J. Godeke, B. J. Bosch, and P. J. Rottier.** 2004. Cleavage inhibition of the murine coronavirus spike protein by a furin-like enzyme affects cell-cell but not virus-cell fusion. J. Virol. **78:**6048–6054.
10. **Delic, J., P. Masdehors, S. Omura, J. M. Cosset, J. Dumont, J. L. Binet, and H. Magdelenat.** 1998. The proteasome inhibitor lactacystin induces apoptosis and sensitizes chemo- and radioresistant human chronic lymphocytic leukaemia lymphocytes to TNF-alpha-initiated apoptosis. Br. J. Cancer **77:**1103–1107.
11. **DeMartino, G. N., and C. A. Slaughter.** 1999. The proteasome, a novel protease regulated by multiple mechanisms. J. Biol. Chem. **274:**22123–22126.
12. **Desterro, J. M., M. S. Rodriguez, and R. T. Hay.** 2000. Regulation of transcription factors by protein degradation. Cell Mol. Life Sci. **57:**1207–1219.
13. **Gao, G., J. Zhang, X. Si, J. Wong, C. Cheung, B. McManus, and H. Luo.** 2008. Proteasome inhibition attenuates coxsackievirus-induced myocardial damage in mice. Am. J. Physiol. Heart Circ. Physiol. **295:**H401–H408.
14. **Groettrup, M., S. Khan, K. Schwarz, and G. Schmidtke.** 2001. Interferon-gamma inducible exchanges of 20S proteasome active site subunits: why? Biochimie **83:**367–372.
15. **Groll, M., L. Ditzel, J. Lowe, D. Stock, M. Bochtler, H. D. Bartunik, and R. Huber.** 1997. Structure of 20S proteasome from yeast at 2.4 Å resolution. Nature **386:**463–471.
16. **Imajoh-Ohmi, S., T. Kawaguchi, S. Sugiyama, K. Tanaka, S. Omura, and H. Kikuchi.** 1995. Lactacystin, a specific inhibitor of the proteasome, induces apoptosis in human monoblast U937 cells. Biochem. Biophys. Res. Commun. **217:**1070–1077.
17. **Kane, R. C., R. Dagher, A. Farrell, C. W. Ko, R. Sridhara, R. Justice, and R. Pazdur.** 2007. Bortezomib for the treatment of mantle cell lymphoma. Clin. Cancer Res. **13:**5291–5294.
18. **Kane, R. C., A. T. Farrell, R. Sridhara, and R. Pazdur.** 2006. United States Food and Drug Administration approval summary: bortezomib for the treatment of progressive multiple myeloma after one prior therapy. Clin. Cancer Res. **12:**2955–2960.
19. **King, R. W., R. J. Deshaies, J. M. Peters, and M. W. Kirschner.** 1996. How proteolysis drives the cell cycle. Science **274:**1652–1659.
20. **Klinger, P. P., and U. Schubert.** 2005. The ubiquitin-proteasome system in HIV replication: potential targets for antiretroviral therapy. Expert Rev. Anti-Infect. Ther. **3:**61–79.
21. **Kropff, M., G. Bisping, E. Schuck, P. Liebisch, N. Lang, M. Hentrich, T. Dechow, N. Kroger, H. Salwender, B. Metzner, O. Sezer, M. Engelhardt,**

H. H. Wolf, H. Einsele, S. Volpert, A. Heinecke, W. E. Berdel, and J. Kienast. 2007. Bortezomib in combination with intermediate-dose dexamethasone and continuous low-dose oral cyclophosphamide for relapsed multiple myeloma. Br. J. Hematol. **138:**330–337.

22. **Kuo, L., G. J. Godeke, M. J. Raamsman, P. S. Masters, and P. J. Rottier.** 2000. Retargeting of coronavirus by substitution of the spike glycoprotein ectodomain: crossing the host cell species barrier. J. Virol. **74:**1393–1406.
23. **La Frazia, S., C. Amici, and M. G. Santoro.** 2006. Antiviral activity of proteasome inhibitors in herpes simplex virus-1 infection: role of nuclear factor-κB. Antivir. Ther. **11:**995–1004.
24. **Luo, H., J. Zhang, C. Cheung, A. Suarez, B. M. McManus, and D. Yang.** 2003. Proteasome inhibition reduces coxsackievirus B3 replication in murine cardiomyocytes. Am. J. Pathol. **163:**381–385.
25. **Maseda, D., S. Meister, K. Neubert, M. Herrmann, and R. E. Voll.** 2008. Proteasome inhibition drastically but reversibly impairs murine lymphocyte development. Cell Death Differ. **15:**600–612.
26. **Nencioni, A., A. Garuti, K. Schwarzenberg, G. Cirmena, G. Dal Bello, I. Rocco, E. Barbieri, P. Brossart, F. Patrone, and A. Ballestrero.** 2006. Proteasome inhibitor-induced apoptosis in human monocyte-derived dendritic cells. Eur. J. Immunol. **36:**681–689.
27. **Nencioni, A., K. Schwarzenberg, K. M. Brauer, S. M. Schmidt, A. Ballestrero, F. Grunebach, and P. Brossart.** 2006. Proteasome inhibitor bortezomib modulates TLR4-induced dendritic cell activation. Blood **108:** 551–558.
28. **Oikawa, T., T. Sasaki, M. Nakamura, M. Shimamura, N. Tanahashi, S. Omura, and K. Tanaka.** 1998. The proteasome is involved in angiogenesis. Biochem. Biophys. Res. Commun. **246:**243–248.
29. **Orlowski, R. Z.** 1999. The role of the ubiquitin-proteasome pathway in apoptosis. Cell Death Differ. **6:**303–313.
30. **Orlowski, R. Z., J. R. Eswara, A. Lafond-Walker, M. R. Grever, M. Orlowski, and C. V. Dang.** 1998. Tumor growth inhibition induced in a murine model of human Burkitt's lymphoma by a proteasome inhibitor. Cancer Res. **58:** 4342–4348.
31. **Pahler, J. C., S. Ruiz, I. Niemer, L. R. Calvert, M. Andreeff, M. Keating, S. Faderl, and D. J. McConkey.** 2003. Effects of the proteasome inhibitor, bortezomib, on apoptosis in isolated lymphocytes obtained from patients with chronic lymphocytic leukemia. Clin. Cancer Res. **9:**4570–4577.
32. **Papandreou, C. N., and C. J. Logothetis.** 2004. Bortezomib as a potential treatment for prostate cancer. Cancer Res. **64:**5036–5043.
33. **Pitts, T. M., M. Morrow, S. A. Kaufman, J. J. Tentler, and S. G. Eckhardt.** 2009. Vorinostat and bortezomib exert synergistic antiproliferative and pro-apoptotic effects in colon cancer cell models. Mol. Cancer Ther. **8:**342–349.

33a. **Raaben, M., C. C. Posthuma, M. H. Verheije, E. G. te Lintelo, M. Kikkert, J. W. Drijfhout, E. J. Snijder, P. J. M. Rottier, and C. A. M. de Haan.** 2010. The ubiquitin-proteasome system plays an important role during various stages of the coronavirus infection cycle. J. Virol. **84:**7869–7879.

34. **Raaben, M., M. J. Groot Koerkamp, P. J. Rottier, and C. A. de Haan.** 2009. Type I interferon receptor-independent and -dependent host transcriptional responses to mouse hepatitis coronavirus infection in vivo. BMC Genomics **10:**350.
35. **Raaben, M., H. J. Prins, A. C. Martens, P. J. Rottier, and C. A. de Haan.** 2009. Non-invasive imaging of mouse hepatitis coronavirus infection reveals determinants of viral replication and spread in vivo. Cell Microbiol. **11:**825–841.
36. **Raaben, M., P. Whitley, D. Bouwmeester, R. A. Setterquist, P. J. Rottier, and C. A. de Haan.** 2008. Improved microarray gene expression profiling of virus-infected cells after removal of viral RNA. BMC Genomics **9:**221.
37. **Read, M. A., A. S. Neish, F. W. Luscinskas, V. J. Palombella, T. Maniatis, and T. Collins.** 1995. The proteasome pathway is required for cytokine-induced endothelial-leukocyte adhesion molecule expression. Immunity **2:**493–506.
38. **Rottier, P. J., M. C. Horzinek, and B. A. van der Zeijst.** 1981. Viral protein synthesis in mouse hepatitis virus strain A59-infected cells: effect of tunicamycin. J. Virol. **40:**350–357.
39. **Satheshkumar, P. S., L. C. Anton, P. Sanz, and B. Moss.** 2009. Inhibition of the ubiquitin-proteasome system prevents vaccinia virus DNA replication and expression of intermediate and late genes. J. Virol. **83:**2469–2479.
40. **Schenkein, D. P.** 2004. Use of proteasome inhibition in the treatment of lung cancer. Clin. Lung Cancer **6**(Suppl. 2)**:**S89–S96.
41. **Shah, S. A., M. W. Potter, T. P. McDade, R. Ricciardi, R. A. Perugini, P. J. Elliott, J. Adams, and M. P. Callery.** 2001. 26S proteasome inhibition induces apoptosis and limits growth of human pancreatic cancer. J. Cell Biochem. **82:**110–122.
42. **Shinohara, K., M. Tomioka, H. Nakano, S. Tone, H. Ito, and S. Kawashima.** 1996. Apoptosis induction resulting from proteasome inhibition. Biochem. J. **317**(Pt. 2)**:**385–388.
43. **Si, X., G. Gao, J. Wong, Y. Wang, J. Zhang, and H. Luo.** 2008. Ubiquitination is required for effective replication of coxsackievirus B3. PLoS One **3:**e2585.
44. **Subklewe, M., K. Sebelin-Wulf, C. Beier, A. Lietz, S. Mathas, B. Dorken, and A. Pezzutto.** 2007. Dendritic cell maturation stage determines susceptibility to the proteasome inhibitor bortezomib. Hum. Immunol. **68:**147–155.
45. **Teale, A., S. Campbell, N. Van Buuren, W. C. Magee, K. Watmough, B. Couturier, R. Shipclark, and M. Barry.** 2009. Orthopoxviruses require a functional ubiquitin-proteasome system for productive replication. J. Virol. **83:**2099–2108.
46. **Tong, Y., J. Qian, Y. Li, H. Meng, and J. Jin.** 2007. The high incidence of varicella herpes zoster with the use of bortezomib in 10 patients. Am. J. Hematol. **82:**403–404.
47. **Verheije, M. H., T. Wurdinger, V. W. van Beusechem, C. A. de Haan, W. R. Gerritsen, and P. J. Rottier.** 2006. Redirecting coronavirus to a nonnative receptor through a virus-encoded targeting adapter. J. Virol. **80:**1250–1260.
48. **Voges, D., P. Zwickl, and W. Baumeister.** 1999. The 26S proteasome: a molecular machine designed for controlled proteolysis. Annu. Rev. Biochem. **68:**1015–1068.
49. **Wang, X., A. Ottosson, C. Ji, X. Feng, M. Nordenskjold, J. I. Henter, B. Fadeel, and C. Zheng.** 2009. Proteasome inhibition induces apoptosis in primary human natural killer cells and suppresses NKp46-mediated cytotoxicity. Haematologica **94:**470–478.
50. **Yu, G. Y., and M. M. Lai.** 2005. The ubiquitin-proteasome system facilitates the transfer of murine coronavirus from endosome to cytoplasm during virus entry. J. Virol. **79:**644–648.
51. **Zou, P., J. Kawada, L. Pesnicak, and J. I. Cohen.** 2007. Bortezomib induces apoptosis of Epstein-Barr virus (EBV)-transformed B cells and prolongs survival of mice inoculated with EBV-transformed B cells. J. Virol. **81:** 10029–10036.